ISSN 0036-0244, Russian Journal of Physical Chemistry A, 2018, Vol. 92, No. 10, pp. 1920–1931. © Pleiades Publishing, Ltd., 2018.

PHYSICAL CHEMISTRY OF SOLUTIONS

Density Functional Theory Study of Solvent Effects on 3-Fluoro-, 3-Chloro-, 3-Bromopyridine[1]

Mustafa Tuğfan Bilkan[a,*]

[a] *Department of Physics, Faculty of Science, Çankırı Karatekin University, Çankırı, 18100 Turkey*

**e-mail: mtbilkan@gmail.com*

Received August 16, 2017

Abstract—Optimized molecular structures and total energies of 3-fluoro-, 3-chloro-, 3-bromopyridine (3-FP, 3-CP, and 3-BP) molecules in vacuum, benzene, toluene, chloroform, dichloromethane, ethanol, dimethylsulfoxide and water media were investigated using DFT/B3LYP-6311++G(*d,p*) method. Moreover, in order to be able to see the effects of changing physical conditions, the thermochemical properties of the structures have been calculated in different temperatures and solvent media. Vibrational frequencies of 3-FP, 3-CP, and 3-BP molecules in vacuum and solvent media were calculated and compared to experimental data from the literature. Also, the chemical reactivities of the structures were calculated from HOMO–LUMO energies. Molecular electrostatic potential maps were plotted and atomic charges of each atom were determined. As a result of the study, it was determined that the molecular parameters of these three structures were slightly influenced by the changing solvent polarity, but the vibration frequencies and other chemical properties have very seriously affected.

Keywords: 3-fluoro-, 3-chloro-, 3-bromopyridine, density functional theory, solvent effects, thermochemical properties, chemical reactivity

DOI: 10.1134/S0036024418100059

INTRODUCTION

Pyridines are important heterocyclic organic compounds in chemistry and especially in biochemistry. They are given by the closed formula C_5H_5N and are found in the structure of many important compounds and ligands. Over the past decade, thousands of scientific articles have been published on pyridine, its derivatives and metal complexes due to their biological and chemical significance. 3-Fluoropyridine (C_5H_4FN, 3-FP), 3-chloropyridine (C_5H_4ClN, 3-CP), and 3-bromopyridine (C_5H_4BrN, 3-BP) are important pyridine derivatives which show bioactivity similar to pyridine. Due to their biological and pharmacological significance, many studies have been made on these molecules, their derivatives and metal complexes [1–3]. The first detailed examination of the vibrational frequencies of 3-FP, 3-CP, and 3-BP molecules was made by Green et all. and the results obtained were published in 1963 [4]. In some studies, it has been determined that derivatives of these molecules exhibit antidepressant and antibacterial properties [5, 6]. On the other hand, many studies have recently been published on the spectroscopic properties of these three structures. Boopalachandran and Laane [7] studied the spectroscopic and structural properties of 2-FP and 3-FP. In 2011, Akalin and Akyüz [8] studied the structure and vibrational properties of free 3-CP and its Zn(II) complexes using spectroscopic methods. Later, Boopalachandran [9] made some researches on vibrational frequencies and structures of 2-CP, 3-CP, 2-BP, and 3-BP.

Although many studies published on the structure and spectroscopic properties of 3-FP, 3-CP, and 3-BP molecules are found in the literature, there is no detailed study on the structural and vibrational properties of these molecules in solvent environments. Examination of solvent effects on molecular structures is very important for computational chemistry applications. Solvents play a very effective role in chemical reactions and can seriously change the structural and vibrational properties of any molecule [10]. In addition, the investigation of solvent effects is pharmacologically important because they can significantly affect the extent of transport, transport, and extent of absorption of living organisms [11].

In this study, solvent effects on the structural and vibrational properties of 3-FP, 3-CP, and 3-BP molecules have been investigated in detail in order to overcome the deficiencies found in the literature. These properties of the molecules have been theoretically investigated in different dielectric media such as benzene (C_6H_6, $\varepsilon = 2.27$), toluene (PhMe, $\varepsilon = 2.37$),

[1] The article is published in the original.

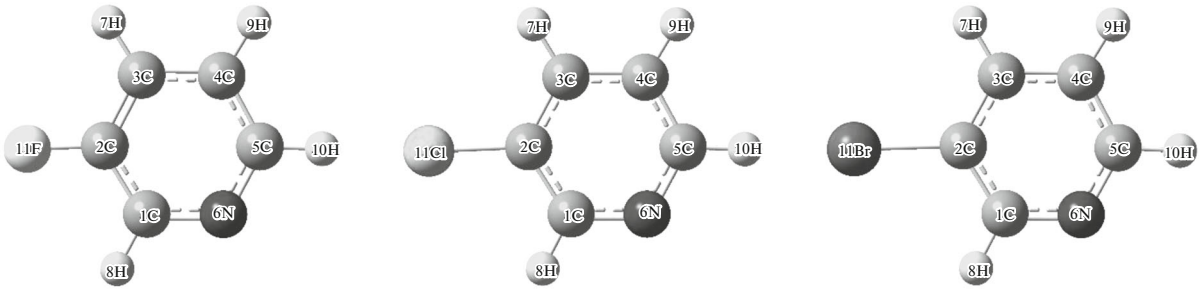

Fig. 1. Optimized molecular structures of 3-FP, 3-CP, and 3-BP in vacuum.

chloroform (CHLF, $\mathscr{E}$ = 4.71), dichloromethane (DCM, $\mathscr{E}$ = 8.93), ethanol (EtOH, $\mathscr{E}$ = 24.85), dimethylsulfoxide (DMSO $\mathscr{E}$ = 46.83), and water (H_2O, $\mathscr{E}$ = 78.36) in addition to the investigations carried out in a vacuum ($\mathscr{E}$ = 1.00) environment.

COMPUTATIONAL METHODS

The DFT/B3LYP method and the 6-311++G(*d,p*) basis set was used for calculate all examined physical and chemical properties of the 3-FP, 3-CP, and 3-BP molecules. All calculations were done on a PC using Gaussian03 [12] and Gaussview [13] programs. Optimizations of 3-FP, 3-CP, and 3-BP molecules was performed in different solvent environments such as vacuum, C_6H_6, PhMe, CHLF, DCM, EtOH, DMSO, and H_2O. The vibrational frequencies were computed in the solvent environments from the optimized structures. In addition, the vibrational frequencies are scaled by 0.98 for 0–1800 cm^{-1} range, 0.96 for 1800–3600 cm^{-1} range [14]. The VEDA4 program [15] were used to characterize the fundamental vibrational modes. Also, entropy and heat capacity values at different temperatures are obtained in solvent environments by using vibrational frequencies.

The electronic properties of the molecules in vacuum and solvent media are calculated from considering total energies and Koopmans' theorem, ionization potential $I = -E_{HOMO}$ and electron affinity $A = -E_{LUMO}$ can be described. Parr et al. [16] explained to chemical potential as $\mu = (E_{HOMO} + E_{LUMO})/2$, chemical hardness as $\eta = (E_{LUMO} - E_{HOMO})/2$ and finally electrophilicity as $\omega = \mu^2/2\eta$.

RESULTS AND DISCUSSIONS

Geometry Optimizations, Energetics, and Thermochemical Properties

The optimized molecular structures of 3-FP, 3-CP, and 3-BP determined by the 6-311++G(*d,p*) basis set are given in Fig. 1. In addition, some calculated important geometric parameters of these three structures in different solvent environments are tabulated in Table 1 together with experimental values from similar structures in the literature [17, 18].

The 3-FP, 3-CP, and 3-BP molecules are closed ring structures and the bonds in the ring plane are not expected to be affected much from the changing solvent environment, generally. For these three structures, the bond lengths expected to be most influenced by the changing solvent medium are 2C-11X (X = F, Cl, Br) outside the ring. As a matter of fact, if Table 1 is examined, the bonds outside the 2C-11X show only 0.001–0.002 Å changes from the vacuum medium to the solvent media while the 2C-11X bonds shows between 0.004 and 0.007 Å. In addition, Table 1 also shows that all calculated geometric parameters are well matched to experimental X-ray diffraction data from the literature.

As expected, there are dramatic differences in C–H bond lengths. As noted in many studies in the literature the reason of this is that because of the low scattering factors of hydrogen atoms in X-ray diffraction, experimental bond lengths of C–H bonds are shorter than the calculated ones. The 1C–2C–11F, 3C–2C–11F, 1C–2C–11Cl, 3C–2C–11Cl, 1C–2C–11Br, and 3C–2C–11Br angles outside the ring were much more severely affected by the changing solvent environment, while very small changes were observed for the angles in the pyridine ring. There is a good agreement between the experimental values from the literature and the values calculated. Since small changes in molecular parameters can cause very serious shifts in the vibration frequencies, these changes in the bond parameters will be very important in studying the vibrational modes.

The calculated total energies and zero-point vibrational energies of 3-FP, 3-CP, and 3-BP structures were given in Table 2 at 298.15 K. As can be seen from the table, all three structures exhibited the same characteristic behavior in changing solvent environments. Decreases were observed in the total and zero-point vibrational energies of the structures as the solvent polarity increased. As a natural and expected result of solvent effects, all structures have a more stable struc-

Table 1. Selected experimental and calculated bond lengths and bond angles of 3-FP, 3-CP, 3-BP in different media

Pyridine	Lengths	Vacuum	C_6H_6	PhMe	CHLF	DCM	EtOH	DMSO	H_2O	Exp.*
3-FP	1C–2C	1.389	1.388	1.388	1.388	1.387	1.387	1.387	1.387	1.366
	1C–6N	1.334	1.336	1.336	1.337	1.338	1.338	1.338	1.338	1.333
	1C–8H	1.086	1.087	1.087	1.088	1.089	1.089	1.089	1.089	0.963
	2C–3C	1.384	1.383	1.383	1.383	1.383	1.383	1.383	1.383	1.409
	2C–11F	1.352	1.355	1.355	1.357	1.358	1.359	1.359	1.359	1.347
3-CP	1C–2C	1.389	1.394	1.394	1.394	1.394	1.393	1.393	1.393	1.372
	1C–6N	1.334	1.335	1.335	1.336	1.336	1.337	1.337	1.337	1.335
	1C–8H	1.086	1.087	1.087	1.088	1.088	1.089	1.089	1.089	0.950
	2C–3C	1.384	1.390	1.390	1.389	1.389	1.390	1.390	1.390	1.374
	2C–11Cl	1.754	1.755	1.755	1.757	1.757	1.758	1.758	1.758	1.739
3-BP	1C–2C	1.389	1.394	1.394	1.394	1.394	1.394	1.394	1.394	1.379
	1C–6N	1.334	1.335	1.336	1.336	1.337	1.338	1.338	1.338	1.331
	1C–8H	1.086	1.086	1.086	1.087	1.088	1.089	1.089	1.089	0.950
	2C–3C	1.384	1.390	1.390	1.390	1.390	1.390	1.390	1.390	1.380
	2C–11Br	1.914	1.915	1.915	1.916	1.917	1.918	1.918	1.918	1.890
	Angles									
3-FP	2C–1C–6N	121.78	121.61	121.60	121.49	121.43	121.38	121.36	121.37	122.55
	2C–1C–8H	120.17	120.27	120.28	120.32	120.36	120.38	120.39	120.36	120.27
	1C–2C–3C	120.94	121.17	121.19	121.31	121.41	121.47	121.49	121.49	120.46
	1C–2C–11F	119.28	119.09	119.08	118.98	118.90	118.84	118.83	118.83	117.12
	3C–2C–11F	119.78	119.74	119.73	119.71	119.69	119.68	119.68	119.68	122.42
	2C–3C–7H	120.48	120.62	120.63	120.71	120.78	120.83	120.85	120.85	123.61
	4C–3C–7H	122.54	122.48	122.48	122.44	122.41	122.39	122.38	122.39	119.89
3-CP	2C–1C–6N	121.78	122.21	122.20	122.12	122.07	122.02	122.01	122.01	122.76
	2C–1C–8H	120.17	120.41	120.42	120.50	120.52	120.53	120.54	120.52	118.59
	1C–2C–3C	120.94	119.90	119.90	120.05	120.11	120.15	120.17	120.18	120.07
	1C–2C–11Cl	119.28	119.63	119.63	119.51	119.47	119.43	119.42	119.42	119.26
	3C–2C–11Cl	119.78	120.48	120.47	120.43	120.42	120.41	120.41	120.40	120.66
	2C–3C–7H	120.48	120.79	120.80	120.92	120.96	121.00	121.02	121.00	121.19
	4C–3C–7H	122.54	121.55	121.54	121.50	121.47	121.45	121.43	121.45	121.11
3-BP	2C–1C–6N	121.78	122.15	122.14	122.04	122.02	121.96	121.97	121.96	122.67
	2C–1C–8H	120.17	120.69	120.70	120.73	120.79	120.80	120.81	120.80	118.63
	1C–2C–3C	120.94	119.92	119.93	120.01	120.10	120.17	120.16	120.17	119.92
	1C–2C–11Br	119.28	119.62	119.61	119.54	119.47	119.42	119.42	119.42	119.08
	3C–2C–11Br	119.78	120.46	120.46	120.45	120.43	120.41	120.42	120.41	121.00
	2C–3C–7H	120.48	121.03	121.04	121.10	121.21	121.25	121.26	121.25	121.17
	4C–3C–7H	122.54	121.30	121.30	121.25	121.20	121.18	121.17	121.18	121.17

* [17, 18].

ture in the solvent environments than in the vacuum environment. A dipole in the molecule will induce a dipole in the medium. The electric field applied to the solute by the solvent dipole will in turn interact with the molecular dipole to lead to net stabilization [19]. While there is not much difference between the ZPVE energies for the 3-FP, 3-CP, and 3-BP in the molecular structure, it appears that there is a very serious difference in total energies.

The calculated entropies and heat capacities of the structures at different temperatures and in different solvent media were also given in Table 3 to see the

Table 2. The calculated total energies (T.E. in Hartree) and zero-point vibrational energies (ZPVE in kcal/mol) of the structures in 298.15 K

Pyridine	Value	Vacuum	C_6H_6	PhMe	CHLF
3-FP	T. E.	−347.61744	−347.62160	−347.62185	−347.62446
	ZPVE	50.27093	50.08202	50.06916	49.93592
3-CP	T. E.	−707.97263	−707.97647	−707.97670	−707.97913
	ZPVE	49.45053	49.28720	49.27676	49.15615
3-BP	T. E.	−2821.89261	−2821.89648	−2821.89671	−2821.89917
	ZPVE	49.07684	48.91650	48.90597	48.78706
		DCM	EtOH	DMSO	H_2O
3-FP	T. E.	−347.62584	−347.62705	−347.62740	−347.62758
	ZPVE	49.86091	49.78996	49.76947	49.76115
3-CP	T. E.	−707.98043	−707.98156	−707.98191	−707.98210
	ZPVE	49.08645	49.02171	49.00348	48.99004
3-BP	T. E.	−2821.90048	−2821.90164	−2821.90198	−2821.90225
	ZPVE	48.72009	48.64802	48.63753	48.61781

effects of temperature and environment changing. The thermochemical properties of the structures were severely affected by the solvent environment and the increased temperature. In calculating the thermal properties of any molecule, contributions come to partition function, entropy, internal energy and constant volume heat capacity from each vibrational mode. Each of the $3N - 6$ (or $3N - 5$ for linear molecules) vibrational modes has a characteristic vibrational temperature. Because these contributions originate from vibrations, the solvent-induced changes in vibrations alter the thermochemical properties [20].

Vibrational Modes and Assignments

Vibrational spectroscopy is a very important instrument for molecular structure studies. Since the vibrations of the atoms forming the molecules cause a characteristic vibration band, very useful information about the molecular structure can be obtained using vibrational spectroscopy. As mentioned in the introduction of this paper, there are many studies in the literature about vibrational properties for 3-FP, 3-CP, and 3-BP molecules. Therefore, experimental IR spectra of these molecules were taken from the literature [21]. In this study, the vibrational frequencies and intensities of 3-FP, 3-CP, and 3-BP were calculated to be very well compatible with the experimental values. In addition, the effects of solvent environments on vibrational frequencies and intensities have been examined in detail. The 3-FP, 3-CP, and 3-BP structures have 11 atoms, and since they are not linear, there are $3N - 6 = 33$ vibration modes (N is the number of atoms). The selected experimental and calculated vibrational modes of 3-FP are given in the Table 4.

Table 4 clearly shows that C–H vibrations are very seriously affected by the changing solvent environment. Also, when Table 4 is examined, it is seen that the vibrational frequencies and intensities calculated in the vacuum environment are very close to the experimental values. The deviations between the experimental and calculated frequencies ranges from 1–21 cm^{-1} for the 0–1800 cm^{-1} region. The solvent environment caused significant shifts in all vibration frequencies and in their intensities. The strongest band seen in the experimental spectrum is 1235 s and this mode is calculated as the strongest IR mode at 1221 cm^{-1}. This mode has assigned as F–C and C–C stretching vibration. This band is the band most affected by the solvent environment, at the same time. The vibrational modes that are least affected by the changing solvent environment are the H–C–C–N, H–C–C, and F–C–C–T torsional modes. Solvent-induced changes at 3000–3100 cm^{-1}, where C–H stretching modes are observed, are much greater than at other sites.

In the Table 5, selected experimental and calculated vibrational modes of 3-CP are given. For the 3-CP structure, Table 5 shows that the vibrations in the C–H region are severely affected by the solvent medium. Also, the environment in which the calculated C–H stretching vibrations are most compatible with the experimental values is the vacuum. When Table 5 is examined, it is seen that the band calculated at 1096 cm^{-1} in vacuum and experimentally at 1107 cm^{-1} is the strongest vibrational mode. It is mainly caused by the Cl–C stretching vibration. This mode is also one of the vibrational modes most affected by the solvent medium. The strong bands observed at 702, 795, 1012, and 1411 cm^{-1} in the exper-

Table 3. The calculated thermochemical properties of the structures in different temperatures and in different media (cal/(mol K))

	Parameters		Vacuum	C_6H_6	PhMe	CHLF	DCM	EtOH	DMSO	H_2O
3-FP	100 K	Entropy	58.196	58.213	58.214	58.225	58.230	58.236	58.237	58.237
		Heat capacity	7.335	7.370	7.372	7.393	7.405	7.415	7.418	7.418
	200 K	Entropy	66.139	66.187	66.190	66.220	66.237	66.252	66.256	66.257
		Heat capacity	12.626	12.680	12.684	12.720	12.739	12.758	12.763	12.765
	298 K	Entropy	73.183	73.198	73.198	73.210	73.218	73.224	73.225	73.227
		Heat capacity	19.200	19.220	19.221	19.236	19.253	19.262	19.264	19.267
	300 K	Entropy	73.315	73.387	73.391	73.438	73.464	73.487	73.493	73.495
		Heat capacity	19.326	19.388	19.392	19.436	19.461	19.484	19.491	19.494
	400 K	Entropy	80.350	80.440	80.446	80.506	80.538	80.569	80.577	80.580
		Heat capacity	25.784	25.847	25.851	25.896	25.922	25.946	25.952	25.957
	500 K	Entropy	87.151	87.255	87.261	87.331	87.369	87.405	87.415	87.419
		Heat capacity	31.209	31.268	31.272	31.314	31.338	31.360	31.367	31.371
3-CP	100 K	Entropy	59.898	59.923	59.925	59.942	59.951	59.960	59.962	59.962
		Heat capacity	8.130	8.166	8.169	8.193	8.205	8.217	8.220	8.221
	200 K	Entropy	68.532	68.586	68.590	68.626	68.645	68.663	68.668	68.669
		Heat capacity	13.682	13.728	13.731	13.763	13.781	13.798	13.802	13.804
	298 K	Entropy	75.967	75.981	75.982	75.992	75.997	76.001	76.002	76.001
		Heat capacity	20.079	20.093	20.094	20.106	20.114	20.121	20.122	20.124
	300 K	Entropy	76.104	76.178	76.183	76.233	76.261	76.286	76.294	76.296
		Heat capacity	20.201	20.254	20.257	20.296	20.318	20.338	20.344	20.348
	400 K	Entropy	83.367	83.457	83.462	83.524	83.558	83.589	83.598	83.602
		Heat capacity	26.492	26.544	26.547	26.586	26.608	26.629	26.635	26.640
	500 K	Entropy	90.311	90.412	90.418	90.488	90.528	90.563	90.572	90.578
		Heat capacity	31.784	31.832	31.835	31.871	31.892	31.911	31.916	31.922
3-BP	100 K	Entropy	62.067	62.104	62.106	62.131	62.146	62.158	62.162	62.163
		Heat capacity	8.787	8.832	8.834	8.863	8.879	8.893	8.897	8.899
	200 K	Entropy	71.195	71.264	71.268	71.314	71.340	71.363	71.369	71.373
		Heat capacity	14.329	14.378	14.381	14.414	14.432	14.449	14.454	14.458
	298 K	Entropy	78.850	78.866	78.867	78.878	78.890	78.881	78.896	78.897
		Heat capacity	20.532	20.544	20.545	20.557	20.563	20.564	20.572	20.577
	300 K	Entropy	78.990	79.079	79.085	79.145	79.179	79.210	79.218	79.224
		Heat capacity	20.651	20.704	20.707	20.745	20.767	20.787	20.793	20.799
	400 K	Entropy	86.363	86.468	86.475	86.546	86.586	86.623	86.633	86.640
		Heat capacity	26.814	26.865	26.869	26.906	26.928	26.949	26.954	26.961
	500 K	Entropy	93.370	93.486	93.493	93.572	93.617	93.659	93.669	93.679
		Heat capacity	32.025	32.072	32.075	32.109	32.130	32.149	32.154	32.161

imental spectrum correspond to calculated strong bands at 703, 792, 1011, and 1421 cm^{-1}, respectively.

Table 6 shows the vibration modes of 3-BP. As in other structures, the strongest vibrational in 3-BP is mode 13, which contains the Br–C stretching vibration. Since the Br atom in the 3-BP structure is a heavier atom than Cl and F in the other structures, it is an expected result that the solvent effects on this structure are more limited. For other constructions, up to 26 cm^{-1} shifts were observed from the vacuum to the water medium in frequencies, while 4 cm^{-1} shifts occurred for the 3-BP structure.

The common result obtained in the study of vibrational modes, as in the comparison of experimental and calculated geometric parameters, is that the changing solvent environment has less influence on

Table 4. Selected experimental and calculated vibrational modes of 3-FP

Mode	Vacuum		C_6H_6		PhMe		CHLF		DCM		EtOH		DMSO		H_2O		Exp.*	PED (%)
	freq.	I_{IR}	freq.	I_{IR}	freq.	I_{IR}	freq.	I_{IR}	freq.	I_{IR}	freq.	I_{IR}	freq.	I_{IR}	freq.	I_{IR}	IR	
7	701	21.8	700	21.4	700	21.4	699	22.2	698	23.0	698	23.9	698	24.2	697	24.2	702m	$\Gamma_{CNCC}(38) + \Gamma_{HCNC}(22) + \Gamma_{CCCC}(19)$
8	801	31.0	802	29.2	802	29.1	802	29.2	802	29.4	802	29.9	802	30.1	802	30.0	799s	$\Gamma_{HCCN}(44) + \Gamma_{HCCC}(17) + \Gamma_{FCCC}(14)$
9	818	12.0	815	13.7	814	13.8	813	15.0	811	15.9	810	16.7	810	16.9	810	17.0	815m	$V_{CC}(46) + V_{FC}(25) + \delta_{CNC}(14)$
13	1017	8.3	1016	8.6	1016	8.6	1015	8.9	1015	9.3	1014	9.5	1014	9.6	1014	9.5	1011w	$\delta_{CCC}(31) + \delta_{CNC}(17) + \delta_{CCN}(15)$
15	1104	9.2	1101	10.0	1101	10.1	1098	10.9	1096	11.4	1095	12.0	1095	12.1	1094	12.2	1085vw	$\delta_{HCC}(54) + V_{NC}(11) + V_{CC}(19)$
16	1195	2.5	1190	3.0	1190	3.1	1187	4.0	1185	4.6	1183	5.7	1183	6.0	1182	6.3	1174sh	$\delta_{HCN}(37) + V_{NC}(19) + \delta_{HCC}(13)$
17	1221	100.0	1210	100.0	1209	100.0	1203	100.0	1198	100.0	1195	100.0	1195	100.0	1195	100.0	1235vs	$V_{FC}(42) + V_{CC}(15) + \delta_{HCN}(12)$
18	1263	2.5	1260	0.8	1260	0.7	1259	0.3	1258	0.1	1258	0.1	1258	0.1	1258	0.1	1254sh	$V_{NC}(56) + V_{CC}(22)$
19	1321	0.8	1318	0.7	1318	0.7	1317	0.7	1315	0.8	1314	0.8	1314	0.8	1313	0.8	1303vw	$\delta_{HCN}(59) + \delta_{HCC}(22)$
20	1435	39.9	1431	42.8	1431	43.1	1429	46.3	1427	48.3	1426	50.5	1426	51.3	1425	51.7	1427s	$\delta_{HCN}(39) + V_{NC}(17) + \delta_{HCC}(10)$
21	1479	45.6	1475	40.0	1475	39.7	1473	37.7	1471	36.5	1470	36.0	1470	35.9	1470	35.6	1478s	$\delta_{HCN}(27) + \delta_{HCC}(26) + V_{CC}(13)$
22	1593	14.1	1589	14.5	1588	14.4	1585	14.0	1583	13.7	1582	13.6	1581	13.6	1581	13.7	1579w	$V_{CC}(46) + \delta_{CCC}(10)$
23	1600	6.6	1600	3.8	1600	3.8	1599	3.4	1600	3.3	1600	3.4	1600	3.4	1599	3.4	1583w	$V_{CC}(32) + V_{NC}(22) + \delta_{CCN}(10)$
26	3081	7.4	3058	2.3	3057	2.2	3039	2.0	3030	2.7	3021	4.0	3018	4.6	3017	4.7	3064w	$V_{CH}(90)$
27	3097	1.2	3070	0.2	3068	0.3	3051	0.9	3042	1.7	3034	2.5	3031	2.7	3030	2.9	3083vw	$V_{CH}(98)$

*[21]; vs is very strong, s is strong, m is medium, w is weak, vw is very weak, V is stretching, δ is bending, Γ is torsional vibration.

Table 5. Selected experimental and calculated vibrational modes of 3-CP

Mode	Vacuum		C_6H_6		PhMe		CHLF		DCM		EtOH		DMSO		H_2O		Exp.*	PED (%)
	freq.	I_{IR}	freq.	I_{IR}	freq.	I_{IR}	freq.	I_{IR}	freq.	I_{IR}	freq.	I_{IR}	freq.	I_{IR}	freq.	I_{IR}	IR	
7	703	50.7	702	51.6	701	51.8	701	55.6	700	58.4	700	61.5	700	62.2	700	63.2	702s	$\Gamma_{CCCC}(36) + \Gamma_{CNCC}(23) + \Gamma_{NCCC}(14)$
8	725	30.7	723	34.8	723	35.8	721	38.8	720	40.6	719	42.4	719	42.8	719	43.4	722m	$\delta_{NCC}(42) + V_{ClC}(24) + \delta_{CNC}(13)$
9	792	56.0	793	54.9	794	55.0	795	57.3	795	59.1	795	61.1	795	61.6	795	62.3	795s	$\Gamma_{HCCC}(43) + \Gamma_{HCCC}(16) + \Gamma_{CCCC}(14)$
11	939	1.0	942	1.0	942	1.0	944	1.0	944	1.0	945	1.0	945	1.0	945	1.1	943vw	$\Gamma_{HCNC}(44) + \Gamma_{HCCC}(41)$
13	1011	66.0	1009	70.9	1009	71.4	1008	77.3	1008	80.1	1008	82.7	1007	83.2	1007	84.0	1012s	$\delta_{CNC}(44) + \delta_{CCC}(30) + \delta_{NCC}(12)$
14	1039	3.9	1036	5.9	1036	6.0	1034	7.4	1033	8.4	1032	9.4	1032	9.5	1032	10.0	1023m	$V_{CC}(54) + V_{NC}(20)$
15	1096	100.0	1093	100.0	1093	100.0	1091	100.0	1090	100.0	1089	100.0	1089	100.0	1088	100.0	1107vs	$V_{ClC}(17) + \delta_{NCC}(17) + \delta_{HCC}(17)$
16	1117	18.2	1114	18.2	1114	18.4	1111	19.5	1110	20.3	1108	21.1	1108	21.3	1107	22.0	1117vs	$\delta_{HCC}(45) + V_{CC}(28)$
17	1199	5.4	1195	5.9	1194	5.9	1192	6.5	1190	6.9	1188	7.3	1188	7.3	1187	7.6	1156w	$\delta_{HCN}(35) + V_{NC}(19) + \delta_{HCC}(14)$
20	1421	61.2	1419	67.7	1418	68.3	1417	75.9	1415	80.7	1414	85.6	1414	86.6	1414	89.2	1411s	$\delta_{HCN}(38) + \delta_{HCC}(11)$
21	1467	50.5	1465	50.8	1465	50.9	1463	52.8	1463	54.0	1462	55.3	1462	55.6	1461	56.2	1462m	$\delta_{HCN}(31) + \delta_{HCC}(24) + V_{NC}(10)$
22	1576	7.9	1573	8.1	1572	8.1	1570	8.7	1569	8.9	1567	9.1	1567	9.2	1567	9.4	1572w	$V_{CC}(29) + V_{NC}(25)$
23	1581	18.0	1580	18.8	1580	18.9	1580	20.3	1580	21.3	1579	22.3	1579	22.5	1579	23.0	1583sh	$V_{CC}(52) + \delta_{CCC}(10)$
26	3080	15.3	3059	4.0	3057	3.6	3040	2.4	3030	3.6	3021	6.0	3018	7.0	3017	7.4	3088w	$V_{CH}(91)$
27	3096	5.3	3071	1.1	3070	1.0	3052	2.4	3042	4.3	3033	6.7	3030	7.5	3029	8.0	3139vw	$V_{CH}(98)$

* [21]; vs is very strong, s is strong, m is medium, w is weak, vw is very weak, V is stretching, δ is bending, Γ is torsional vibration.

Table 6. Selected experimental and calculated vibrational modes of 3-BP

Mode	Vacuum		C_6H_6		PhMe		CHLF		DCM		EtOH		DMSO		H_2O		Exp.*	PED (%)
	freq.	I_{IR}	freq.	I_{IR}	freq.	I_{IR}	freq.	I_{IR}	freq.	I_{IR}	freq.	I_{IR}	freq.	I_{IR}	freq.	I_{IR}	IR	
7	700	48.91	699	46.63	699	31.55	698	31.94	697	32.39	696	32.83	696	32.82	695	32.88	697vs	$\Gamma_{CCCC}(36) + \Gamma_{CNCC}(25) + \Gamma_{NCCC}(13)$
8	701	29.33	699	31.02	699	46.17	698	47.45	698	48.01	698	48.77	697	49.66	697	50.61	700vs	$\delta_{NCC}(44) + V_{BrC}(21) + \delta_{CNC}(15)$
9	788	59.28	789	54.21	789	54.06	790	52.99	791	52.82	792	53.94	791	53.32	791	53.57	787vs	$\Gamma_{HCCN}(43) + \Gamma_{HCCC}(17) + \Gamma_{CCCC}(14)$
12	975	0.12	980	0.12	980	0.12	982	0.13	984	0.13	986	0.13	985	0.13	985	0.13	971vw	$\Gamma_{HCNC}(35) + \Gamma_{HCCN}(30) + \Gamma_{HCCC}(11)$
13	1004	100.00	1003	100.00	1003	100.00	1002	100.00	1001	100.00	1000	100.00	1000	100.00	1000	100.00	1004vs	$\delta_{CCC}(42) + V_{BrC}(34) + \delta_{CNC}(26)$
14	1036	1.89	1033	2.56	1033	2.62	1031	3.14	1031	3.15	1029	3.44	1029	3.49	1029	3.85	1023m	$V_{CC}(50) + V_{NC}(17)$
15	1081	66.11	1080	60.07	1079	59.74	1078	55.77	1077	52.75	1077	51.10	1076	50.49	1076	50.18	1089s	$\delta_{HCC}(26) + \delta_{NCC}(20) + V_{BrC}(10)$
16	1116	12.39	1114	13.07	1113	13.13	1111	13.71	1110	14.08	1109	14.45	1108	14.54	1107	14.58	1114m	$\delta_{HCC}(41) + V_{CC}(24)$
17	1199	5.43	1195	5.44	1195	5.45	1192	5.59	1190	5.70	1189	5.70	1188	5.84	1188	5.98	1191w	$\delta_{HCN}(34) + V_{NC}(19) + \delta_{HCC}(14)$
20	1419	59.05	1416	60.77	1416	60.96	1414	63.71	1413	65.25	1412	67.41	1412	67.64	1411	69.07	1414s	$\delta_{HCN}(40) + \delta_{HCC}(10)$
21	1464	45.77	1462	43.88	1462	43.82	1461	43.35	1460	42.67	1459	42.89	1459	42.68	1459	42.87	1465s	$\delta_{HCN}(32) + \delta_{HCC}(24) + V_{CC}(11)$
22	1569	7.48	1566	7.50	1566	7.50	1563	7.53	1562	7.58	1560	7.83	1560	7.62	1560	7.73	1574m	$V_{NC}(24) + V_{CC}(21)$
23	1578	21.37	1577	20.98	1577	20.99	1576	21.29	1577	21.61	1576	21.73	1576	22.19	1576	22.65	1578m	$V_{CC}(50) + \delta_{CCC}(12)$
26	3080	16.63	3058	3.74	3057	3.37	3041	1.99	3031	2.99	3019	5.22	3019	5.81	3017	6.12	3051w	$V_{CH}(90)$
27	3096	5.62	3071	1.52	3070	1.48	3053	2.58	3042	4.37	3031	6.29	3030	7.15	3028	7.76	3064w	$V_{CH}(98)$

* [21]; vs is very strong, s is strong, m is medium, w is weak, vw is very weak, V is stretching, δ is bending, Γ is torsional vibration.

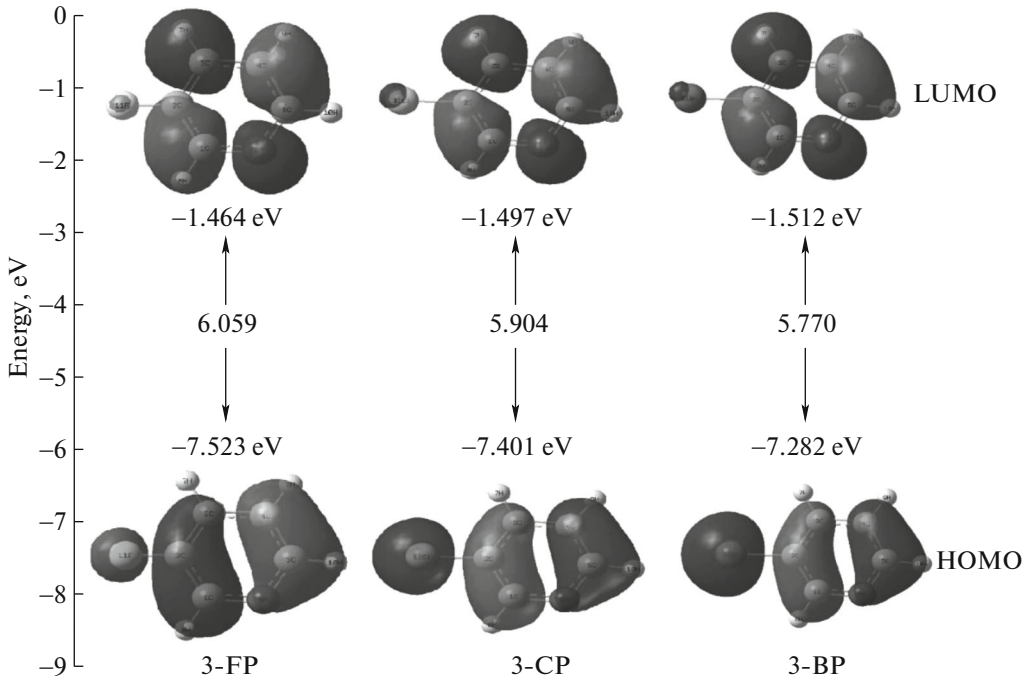

Fig. 2. HOMO–LUMO contour maps and energy gaps of 3-FP, 3-CP, and 3-BP in vacuum.

the movements of the atoms and bonds in the plane of the ring. Changing solvent environment have much more serious effects on the vibrations of C–H and C–X (X = F, Cl, Br) atoms. Tables 4–6 confirm these results. Changes in vibration modes are important when moving from gas to solution.

HOMO–LUMO Energies and Chemical Reactivity

In this study, we have also computed the highest occupied molecular orbital (HOMO) energies, lowest unoccupied molecular orbital (LUMO) energies and their energy gaps for 3-FP, 3-CP, and 3-BP. HOMO and LUMO energies are important parameters in computational chemistry because they help define many physical and chemical properties. The energy gap between HOMO–LUMO is a considerable parameter in determining molecular electrical transport properties. the energy of the HOMO is directly related to the ionization potential, and LUMO energy is directly related to the electron affinity. This is also used by the frontier electron density for estimating the most reactive position in *p*-electron systems and also explains several types of reaction in conjugated system [22].

In Table 7 calculated dipole moments and chemical reactivities of the structures in different dielectric media are seen. It is seen that increasing the dielectric constant causes regular change in HOMO and LUMO energies. Similarly, the dipole moments of the structures increases regularly with increasing dielectric constant. Larger dipole moments cause greater stabilization in solution phase. At the same time, changing solvent polarity directly affects chemical reactivity in Table 7. The HOMO–LUMO contour maps of 3-FP, 3-CP, and 3-BP were given in Fig. 2. The positive parts are represented in red and negative parts are represented in green color. Moreover, for the 3-FP, HOMO shows bonding character between 1C–2C–3C and 4C–5C–6N atoms. LUMO shows bonding character between 2C–1C–8H, 5C–4C–9H, and 7H–3C atoms. For the 3-CP and 3-BP, the same bonding and antibonding characters are available. In Fig. 2, it is noticeable that 11Cl and 11Br atoms are positive while 11F1 is negative. The energy gap between HOMO–LUMO decreases from 3-FP to 3-BP.

Molecular Electrostatic Potential

Molecular electrostatic potential (MEP) maps are drawings that visualize the distribution of charge on the molecule in three dimensions. These maps give the shape, size and charge distribution of a molecule. Generally, the red regions in the map give low electrostatic potential energy and low electronegativity, while the blue regions symbolize high electrostatic potential energy and high electronegativity. MEP maps also provide important information about the nature of molecular bonds. They say a lot about the difference in electronegativity.

To predict reactive sites of electrophilic and nucleophilic attack for 3FP, 3-CP, and 3-BP, MEPs were calculated and in Fig. 3, molecular electrostatic potential surface contour maps of 3FP, 3-CP, and

Table 7. Calculated chemical reactivity (eV) and dipole moments of the structures in different media

	Parameters	Vacuum	C_6H_6	PhMe	CHLF	DCM	EtOH	DMSO	H_2O
3-FP	E_{LUMO}	−1.464	−1.410	−1.408	−1.391	−1.388	−1.385	−1.385	−1.383
	E_{HOMO}	−7.523	−7.471	−7.469	−7.451	−7.447	−7.443	−7.443	−7.440
	$\Delta E_{LUMO-HOMO}$	6.059	6.061	6.061	6.060	6.060	6.059	6.058	6.057
	Electron affinity (A)	1.464	1.410	1.408	1.391	1.388	1.385	1.385	1.383
	Ionization potential (I)	7.523	7.471	7.469	7.451	7.447	7.443	7.443	7.440
	Global hardness (η)	3.029	3.031	3.031	3.030	3.030	3.029	3.029	3.028
	Chemical potential (μ)	−4.493	−4.441	−4.439	−4.421	−4.417	−4.414	−4.414	−4.411
	Electrophilicity (ω)	3.332	3.253	3.250	3.225	3.220	3.216	3.216	3.213
	μ, D	2.187	2.554	2.577	2.818	2.952	3.071	3.106	3.121
3-CP	E_{LUMO}	−1.497	−1.438	−1.436	−1.420	−1.414	−1.412	−1.412	−1.408
	E_{HOMO}	−7.401	−7.352	−7.350	−7.338	−7.334	−7.332	−7.332	−7.328
	$\Delta E_{LUMO-HOMO}$	6.035	5.914	5.914	5.918	5.919	5.920	5.920	5.919
	Electron affinity (A)	1.366	1.438	1.436	1.420	1.414	1.412	1.412	1.408
	Ionization potential (I)	7.401	7.352	7.350	7.338	7.334	7.332	7.332	7.328
	Global hardness (η)	3.017	2.957	2.957	2.959	2.960	2.960	2.960	2.960
	Chemical potential (μ)	−4.383	−4.395	−4.393	−4.379	−4.374	−4.372	−4.372	−4.368
	Electrophilicity (ω)	3.184	3.266	3.263	3.240	3.232	3.228	3.229	3.223
	μ, D	2.165	2.530	2.553	2.798	2.931	3.051	3.087	3.102
3-BP	E_{LUMO}	−1.512	−1.449	−1.447	−1.429	−1.424	−1.423	−1.422	−1.419
	E_{HOMO}	−7.281	−7.238	−7.237	−7.232	−7.225	−7.224	−7.225	−7.221
	$\Delta E_{LUMO-HOMO}$	5.770	5.789	5.790	5.803	5.801	5.801	5.803	5.802
	Electron affinity (A)	1.512	1.449	1.447	1.429	1.424	1.423	1.422	1.419
	Ionization potential (I)	7.281	7.238	7.237	7.232	7.225	7.224	7.225	7.221
	Global hardness (η)	2.885	2.894	2.895	2.902	2.900	2.901	2.902	2.901
	Chemical potential (μ)	−4.397	−4.344	−4.342	−4.330	−4.325	−4.323	−4.323	−4.320
	Electrophilicity (ω)	3.350	3.259	3.256	3.231	3.224	3.222	3.221	3.217
	μ, D	2.144	2.508	2.531	2.772	2.909	3.029	3.065	3.089

3-BP in vacuum and water media are drawn. As can see from the Fig. 3, full red or full blue colors are dominant on the MEP map. Particularly, nitrogen atoms of the molecules have mostly red regions and hydrogen atoms have blue colors, which indicates that the difference in electronegativity is high. As expected, positive charge densities are localized on hydrogen atoms. Cl and Br atoms have gray colors while the F atom has yellow region. In this case, we can say that negative charge density is localized on F atom.

CONCLUSIONS

In this study, for the 3-fluoro-, 3-chloro-, 3-bromopyridine, some physical and chemical properties have been examined in vacuum, C_6H_6, PhMe, CHLF, DCM, EtOH, DMSO, and H_2O media. Total energies, optimized molecular structures, entropies and heat capacities at different temperatures, HOMO–LUMO energies and chemical reactivities were calculated. The vibrational frequencies of the structures in vacuum and solvent environments were calculated and compared with the experimental data from the literature. In addition, molecular electrostatic potential maps for 3-FP, 3-CP, and 3-BP were drawn and atomic charges were determined. The following conclusions were reached at the end of the study.

• It has been determined that the changing solvent environments has limited effects on the molecular parameters of these three structures. Particularly, the bond lengths and bond angles remaining in the ring planes are little affected by the changing solvent media. However, the calculated molecular parameters are quite compatible with the experimental data available in the literature.

• The increased polarity of the environment and the increased temperature increase the entropy and heat capacities of the structures.

• The calculated vibrational frequencies and intensities for the three structures are very compatible with

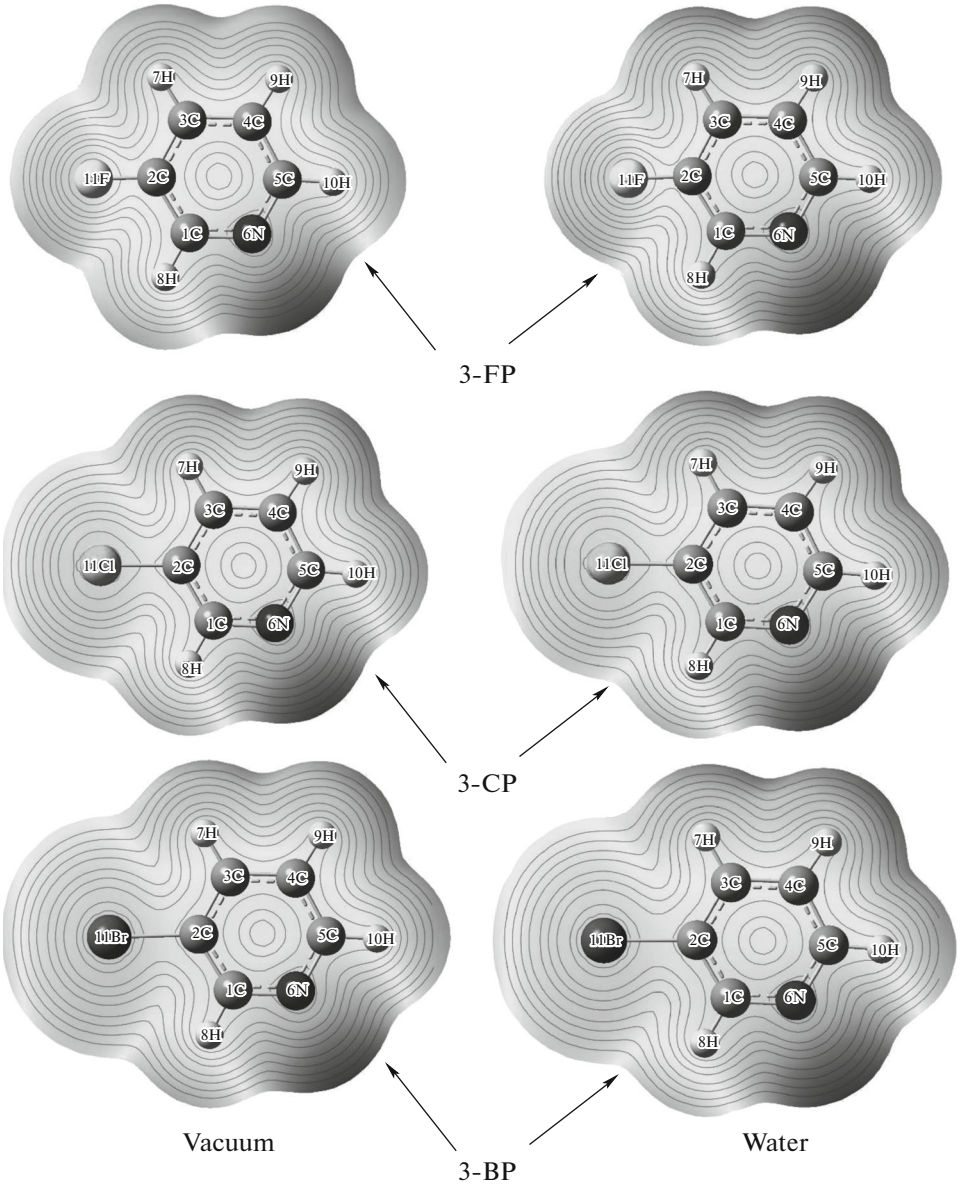

Fig. 3. Molecular electrostatic potential surface contour maps of 3FP, 3-CP, and 3-BP in vacuum and water media.

the experimental data from the literature. Although the changing solvent environments has little effect on the molecular structures, they have serious effects on vibration frequencies and their intensities. Especially, C–H vibrations are greatly influenced by environments changes.

• The changing solvent environments also change the electron affinities, ionization potentials, global hardness, chemical potentials, electrophilicity and dipole moments for 3-FP, 3-CP, and 3-BP.

ACKNOWLEDGMENTS

This study was funded by the Çankırı Karatekin University Scientific Research Fund (project no. EFF20217B33).

REFERENCES

1. W. R. Dolbier and Y. L. Xu, J. Fluorine Chem. **123**, 71 (2003).
2. Y. Nibu, R. Marui, and H. Shimada, Chem. Phys. **442**, 7 (2007).
3. S. Wöhlert, I. Jess, and C. Nather, Inorg. Chem. Acta **407**, 243 (2013).
4. H. S. Green, W. Kynaston, and H. M. Paisly, Spectrochim. Acta **19**, 549 (1963).
5. W. S. Saari, W. Halczenko, S. W. King, J. R. Huff, J. P. Guare, C. A. Hunt, W. C. Randall, P. S. Anderson, V. J. Lotti, D. A. Taylor, and B. V. Clinechmidt, J. Med. Chem. **26**, 1696 (1983).
6. T. Miyamoto, H. Egawa, and J. Matsumoto, Chem. Pharm. Bull. **35**, 2280 (1987).

7. P. Boopalachandran and J. Laane, Spectrochim. Acta. A. **79**, 1191 (2011).
8. E. Akalin and S. Akyüz, J. Mol. Struct. **993**, 390 (2011).
9. P. Boopalachandran, H. L. Sheu, and J. Laane, J. Mol. Struct. **1023**, 61 (2012).
10. M. Orozco and F. J. Luque, Chem. Rev. **100**, 4187 (2000).
11. M. A. Halim, D. M. Shaw, and R. A. Poirier, J. Mol. Struct.: THEOCHEM **960**, 63 (2010).
12. M. J. Frisch, G. W. Trucks, H. B. Schlegel, G. E. Scuseria, M. A. Robb, J. R. Cheeseman, J. A. Montgomery, Jr., T. Vreven, K. N. Kudin, J. C. Burant, et al., *Gaussian 03, Revision D.01* (Gaussian Inc., Wallingford, CT, 2004).
13. R. D. Dennington, T. A. Keith, and J. M. Millam, *GaussView 5* (Gaussian Inc., 2008).
14. N. Sundaraganesan, G. Elango, S. Sebastian, and P. Subramani, Indian J. Pure Appl. Phys. **47**, 481 (2009).
15. M. H. Jamroz, *Vibrational Energy Distribution Analysis VEDA 4* (Warsaw, 2004).
16. R. G. Parr, J. Am. Chem. Soc. **121**, 1922 (1999).
17. V. Vasylyeva, O. V. Shishkin, A. V. Maleev, and K. Merz, Cryst. Growth Des. **12**, 1032 (2012).
18. F. M. A. Noa, S. A. Bourne, H. Su, E. Weber, and L. R. Nassimbeni, Cryst. Growth Des. **16**, 4765 (2016).
19. L. Qiu, X. H. Ju, and H. M. Xiao, J. Chin. Chem. Soc.-Taip. **52**, 405 (2005).
20. J. W. Ochterski, *Thermochemistry in Gaussian* (Gaussian Inc., 2000).
21. http://webbook.nist.gov/cgi/inchi?ID=C372474&Mask=80.
22. R. Shahidha, A. A. Al-Saadi, and S. Muthu, Spectrochim. Acta, A **134**, 127 (2015).